Minimum reflux calculation for multicomponent distillation in multi-feed, multi-product columns: Algorithm, Implementation, and Case Studies

Zheyu Jiang[⋆1,3], Mohit Tawarmalani[*2], and Rakesh Agrawal[†1]

[1]Davidson School of Chemical Engineering, Purdue University, West Lafayette, IN 47907
[2]Mitch Daniels School of Business, Purdue University, West Lafayette, IN 47907
[3]School of Chemical Engineering, Oklahoma State University, Stillwater, OK 74078

Corresponding authors: zjiang@okstate.edu[⋆], mtawarma@purdue.edu[*], agrawalr@purdue.edu[†]

Abstract

In this work, we present the first algorithm for identifying the minimum reboiler vapor duty requirement for a general multi-feed, multi-product (MFMP) distillation column separating ideal multicomponent mixtures. This algorithm incorporates our latest advancement in developing the first shortcut model for MFMP columns. By comparing with rigorous Aspen Plus simulations, we demonstrate the accuracy and efficiency of this algorithm through case studies. The results obtained from these case studies also provide valuable insights on optimal design of multicomponent distillation systems as well as the minimum reflux behavior for MFMP columns. Counterintuitive at first glance, many of these insight are against the design guidelines and heuristics that chemical engineering community has been adopting for decades. We find out, for example, that placing a colder feed stream above a hotter feed stream sometimes leads to higher energy requirement. Furthermore, decomposing a general MFMP column into individual simple columns to estimate the minimum reflux ratio for the MFMP column, which is the common underlying assumption in existing formulations for optimizing multicomponent distillation systems, may lead to incorrect results. Thus, the algorithm presented in here offers the first fast, accurate, and automated approach that can be easily incorporated in an optimization framework to synthesize and design new, energy-efficient, and cost-effective multicomponent distillation systems.

Keywords: Multicomponent distillation, multi-feed and multi-product distillation column, minimum reflux ratio, Underwood method, optimization

1 Introduction

Distillation is an ubiquitous separation technology in the chemical process industries, consuming almost 50% of the energy used by the chemical industries and about 40% by the refining process[1]. Assuming that 50% of the CO_2 equivalent release from process heating in chemical manufacturing and 40% in petroleum refining are attributable to distillation, distillation alone will be responsible for 95 million tons of CO_2 release in the U.S. each year[2]. Thus, to decarbonize the U.S. manufacturing sector, it is essential to significantly reduce the energy consumption and carbon footprint of distillation process[3].

While binary mixtures can generally be separated using one distillation column, multicomponent mixtures, which are more commonly encountered in industrial separations, require a sequence of distillation columns called a distillation configuration to achieve the desired separation. As the number of components in the feed increases, the total number of possible distillation configurations increases combinatorially[4]. Among these distillation configurations, many of them contain one or more distillation columns with multiple feed streams and/or one or more sidedraw product streams. And it is well-known that these configurations with multi-feed, multi-product (MFMP) columns are generally more energy-efficient to operate than the so called "sharp-split configurations" which do not involve any MFMP column[5;6].

MFMP columns can also be derived from conventional one-feed, two-product columns in binary and multicomponent distillation by applying various process intensification techniques[7–9], including heat pumps[10;11], double and multi-effect[12], intermediate reboilers and condensers[13], prefractionator arragement[14], feed preconditioning[15], heat and mass integration[16], and so on. Compared to the original conventional columns, these news MFMP columns not only require significantly less energy from a first-law of thermodynamics perspective, but also have much higher thermodynamic efficiency from a second-law perspective[17], making them more attractive than alternative technologies (e.g., membranes) for a variety of industrial separations[9;18]. Furthermore, when heat pumps are used in conjunction with other techniques above, the resulting MFMP columns can now be flexibly powered by alternative energy sources (e.g., renewable electricity such as solar and wind). Thus, MFMP columns are becoming increasingly important in the context of industrial decarbonization and net-zero economy, as they can revamp conventional steam-driven distillation systems whose energy primarily comes from fossil fuel combustion[2].

The minimum reflux ratio of a distillation column is closely related to its energy consumption, capital cost, and operational limit[19;20], hence it is a key parameter in distillation design and operation. The naive approach of determining a column's minimum reflux ratio involves performing exhaustive sensitivity analysis using process simulators, which is a tedious task that often faces convergence issues. As a result, a fast and accurate algorithmic approach to calculate the actual minimum reflux condition of a general MFMP column is critical for designing new, energy-efficient, and cost-effective multicomponent distillation systems. Ideally, such a method should also have a simple mathematical formulation that can be easily incorporated in a (global) optimization framework for fast and accurate identification of attractive configurations from an enormous configuration search space.

Over the past decades, a number of algorithmic methods have been proposed to determine the minimum reflux ratio of a general MFMP column accurately and efficiently. A comprehensive review of these methods can be found in the first article of this series[21]. However, these methods either rely on several simplifying assumptions, some of which turn out to be too restrictive or even incorrect as we will later demonstrate, or they require rigorous tray-by-tray calculations which are computationally expensive to perform and thus impractical to be implemented for solving complex MFMP columns. To fill the gap between existing methods and what practitioners anticipate, in our previous work[21], we develop the first shortcut mathematical model to analytically determine the minimum reflux ratio of any general MFMP column entirely based on the assumptions of ideal vapor-liquid equilibrium, constant relative volatility, as well as constant molar overflow for every component. No additional restrictions on the particular configuration of the MFMP column or its product specifications are needed. Also, the proposed shortcut model does not involve any tray-by-tray calculations. Furthermore, the physical and mathematical properties associated with the shortcut model are explored, from which we successfully derive the mathematical conditions for

any general MFMP column operated at minimum reflux.

Continuing our previous work, in this article, we introduce an algorithmic method that incorporates the shortcut model developed earlier to efficiently and accurately determine the minimum reboiler vapor duty requirement for a general MFMP column separating a multicomponent mixture. This algorithm can either be used by itself to find the minimum reflux condition for a standalone MFMP column, or can be embedded into a global optimization framework[6;17;22;23] to simultaneously optimize an entire configuration consisting of one or more MFMP columns. Later, we present three case studies in comparison with rigorous Aspen Plus simulations to illustrate the accuracy and usefulness of our algorithm. Also, these case studies are carefully designed to challenge some of the widely-used design heuristics and rules-of-thumb researchers and industrial practitioners have been relying upon. The shortcut method and the minimum reflux calculation algorithm presented in this series thus provide new perspectives on how to accurately model, design, and operate MFMP columns.

2 A Brief Summary of Shortcut Model for MFMP Columns

Before we introduce the algorithm formulation for determining the minimum reflux condition of a MFMP column, we present a high-level review of the shortcut model and some of the key results during its derivation, including the mathematical conditions that dictate whether the target separation task can be achieved (with finite or inifite number of stages) in the MFMP column. We consider a column section, which is separated by either a feed or a product stream, as the smallest module of a MFMP column. From this, we can derive algebraic constraints that must be satisfied for each and every pair of adjacent column sections to maintain feasibility of separation. In particular, when the target separation cannot be achieved without requiring an infinite number of stages (i.e., some column sections are pinched), then the corresponding reflux ratio is the minimum reflux ratio of the MFMP column with respect to the target separation goal. We encourage readers to refer back to our previous work[21] for detailed derivations and explanation of the results summarized below.

Consider a MFMP column with N_{SEC} column sections separated by N_{F} feed and N_{W} streams (note that $N_{\mathrm{SEC}} = N_{\mathrm{F}} + N_{\mathrm{W}} + 1$). Following the nomencalture used in our previous work[21], for a c-component system, let $\mathcal{C} = \{1, \ldots, c\}$ and $\alpha_c > \alpha_{c-1} > \cdots > \alpha_1 = 1$ be the relative volatilities with respect to the least volatile one (component 1). Given the feed and product specifications, we can determine the net material upward flow for component i in every column section k, namely $d_i^{\mathrm{SEC}_k}$. Then, for a specific section vapor flow V^{SEC_k} where k is numbered from top ($k = 1$) to bottom ($k = N_{\mathrm{SEC}}$), we can solve the following equation[21] to obtain a total of c roots, $\{\gamma_i^{\mathrm{SEC}_k}\}_{i\in\mathcal{C}}$:

$$\sum_{i=1}^{c} \frac{\alpha_i d_i^{\mathrm{SEC}_k}}{\alpha_i - \gamma^{\mathrm{SEC}_k}} = V^{\mathrm{SEC}_k}. \tag{1}$$

Suppose $d_c, \ldots, d_l > 0$, $d_{l-1}, \ldots, d_{h+1} = 0$, and $d_h, \ldots, d_1 < 0$ for some $1 \le h < l \le c-1$ in a column section. It can be verified that, among all c roots, $c-1$ of them lie in the following intervals:

$$\begin{aligned} \gamma_i^{\mathrm{SEC}_k} &\in (\alpha_i, \alpha_{i+1}) && \text{for } i \in \{1, \ldots, h\} \\ \gamma_i^{\mathrm{SEC}_k} &= \alpha_i && \text{for } i \in \{h+1, \ldots, l-1\} \\ \gamma_{i+1}^{\mathrm{SEC}_k} &\in (\alpha_i, \alpha_{i+1}) && \text{for } i \in \{l, \ldots, c-1\}. \end{aligned} \tag{2}$$

The remaining root, which is referred to as the pinch root $\gamma_p^{\mathrm{SEC}_k}$, turns out to be closely related to the actual pinch zone composition in section k. When $1 \le h < l \le c-1$, it can be shown that $\gamma_p^{\mathrm{SEC}_k} = \gamma_l^{\mathrm{SEC}_k} \in (\alpha_{l-1}, \alpha_l) \subset (\alpha_h, \alpha_l)$ (i.e., the l^{th} smallest root of Equation (1)). In this case, the pinch index $p^{\mathrm{SEC}_k} = l$. For example, consider a five-component system ($c = 5$). Suppose $d_1^{\mathrm{SEC}_k}, \ldots, d_3^{\mathrm{SEC}_k} < 0$ and $d_4^{\mathrm{SEC}_k}, d_5^{\mathrm{SEC}_k} > 0$ (see Figure 1). Then, the pinch index $p^{\mathrm{SEC}_k} = 4$. In terms of the edge cases beyond $1 \le h$ or $l \le c-1$, when $d_i < 0$ for all $i \in \mathcal{C}$, we set $h = c-1$ and $l = c$ and thus $\gamma_p^{\mathrm{SEC}_k} = \gamma_c^{\mathrm{SEC}_k} > \alpha_c$. In this case, the pinch index $p^{\mathrm{SEC}_k} = c$. When $d_i > 0$ for all $i \in \mathcal{C}$, we set $h = 0$ and $l = 1$ and thus $\gamma_p^{\mathrm{SEC}_k} = \gamma_1^{\mathrm{SEC}_k} < \alpha_1 = 1$. In this case, the pinch index $p^{\mathrm{SEC}_k} = 1$.

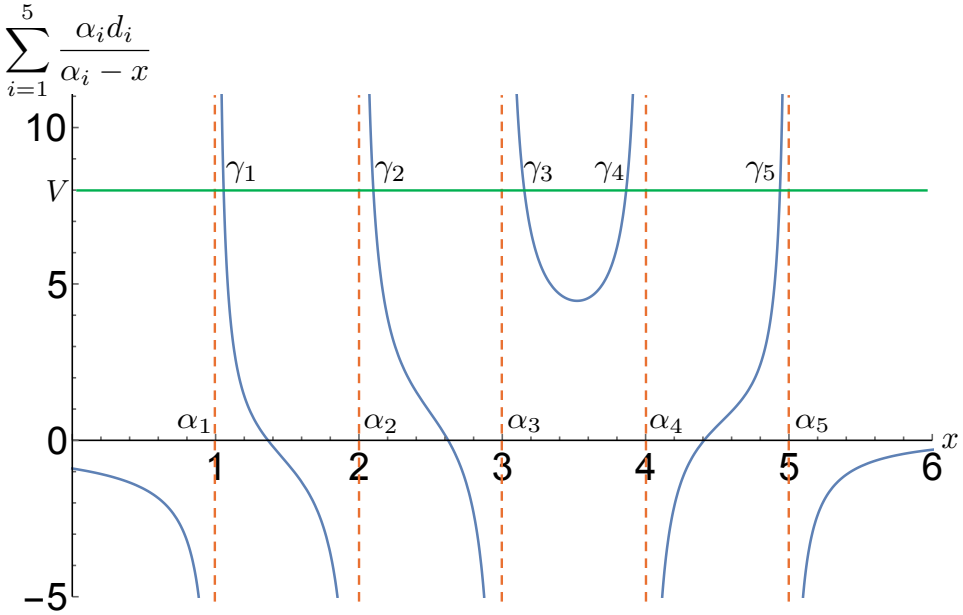

Figure 1: Roots of Equation (1) for an illustrative example, in which $(d_1, d_2, d_3, d_4, d_5) = (-0.5, -0.4, -0.3, 0.2, 0.1)$ and $(\alpha_1, \alpha_2, \alpha_3, \alpha_4, \alpha_5) = (1, 2, 3, 4, 5)$. The section vapor flow V is set to be 8. In this case, γ_4 is the pinch root and thus the pinch index is 4.

When two adjacent column sections are separated by a feed stream F_j ($j = 1, \ldots, N_{\mathrm{F}}$), we denote the section above F_j as $\mathrm{TOP}_{\mathrm{F}j}$ and the one below as $\mathrm{BOT}_{\mathrm{F}j}$. Since $d_i^{\mathrm{TOP}_{\mathrm{F}j}} \ge d_i^{\mathrm{BOT}_{\mathrm{F}j}}$ for every component $i \in \mathcal{C}$, we can show that the pinch indices satisfy $p^{\mathrm{TOP}_{\mathrm{F}j}} \le p^{\mathrm{BOT}_{\mathrm{F}j}}$. Thus, an index set $\mathcal{I}_{\mathrm{F}_j}$ is defined for this feed F_j as:

$$\mathcal{I}_{\mathrm{F}_j} = \{i \in \mathcal{C} | \gamma_i^{\mathrm{TOP}_{\mathrm{F}j}} > \gamma_p^{\mathrm{TOP}_{\mathrm{F}j}}, \gamma_{i-1}^{\mathrm{BOT}_{\mathrm{F}j}} < \gamma_p^{\mathrm{BOT}_{\mathrm{F}j}}\} = \{p^{\mathrm{TOP}_{\mathrm{F}j}} + 1, \ldots, p^{\mathrm{BOT}_{\mathrm{F}j}}\}. \tag{3}$$

For example, consider the same five-component system discussed above where root profile shown in Figure 1 corresponds to the lower section of feed stream F_j. Now, for the upper section, suppose $d_1^{\mathrm{TOP}_{\mathrm{F}j}} < 0$ and $d_2^{\mathrm{TOP}_{\mathrm{F}j}}, \ldots, d_5^{\mathrm{TOP}_{\mathrm{F}j}} > 0$. Following the same reasonings above, the pinch index for section $\mathrm{TOP}_{\mathrm{F}j}$ is $p^{\mathrm{TOP}_{\mathrm{F}j}} = 2$. Thus, $\mathcal{I}_{\mathrm{F}_j} = \{3, 4\}$. With this, one of the key results we obtained in our previous work[21] is that, the feasibility of the target separation in sections $\mathrm{TOP}_{\mathrm{F}j}$ and $\mathrm{BOT}_{\mathrm{F}j}$ requires the following γ root constraint to be satisfied for every $i \in \mathcal{I}_{\mathrm{F}_j}$:

$$\gamma_i^{\mathrm{TOP}_{\mathrm{F}j}} \ge \rho_{i-1,\mathrm{F}_j} \ge \gamma_{i-1}^{\mathrm{BOT}_{\mathrm{F}j}} \qquad \forall i \in \mathcal{I}_{\mathrm{F}_j};\ j = 1, \ldots, N_{\mathrm{F}} \tag{4}$$

where the equality holds when the two column sections are pinched and $\{\rho_{i-1,\mathrm{F}_j}\}_{i\in\mathcal{I}_{\mathrm{F}_j}}$ are a subset of solutions of the following equation:

$$\sum_{m=1}^{c}\frac{\alpha_m l_{m,\mathrm{F}_j}}{\alpha_m-\rho_{i,\mathrm{F}_j}}=0 \qquad \text{or} \qquad \sum_{m=1}^{c}\frac{\alpha_m f_{m,\mathrm{F}_j}}{\alpha_m-\rho_{i,\mathrm{F}_j}}=V_{\mathrm{F}_j} \qquad i=1,\ldots,c-1;\ j=1,\ldots,N_{\mathrm{F}}, \tag{5}$$

where $\rho_{i,\mathrm{F}_j}\in(\alpha_i,\alpha_{i+1})$. Here, $l_{m,\mathrm{F}_j}\geq 0$, $f_{m,\mathrm{F}_j}\geq 0$, and $V_{\mathrm{F}_j}\geq 0$ correspond to the flow rate of component m in the liquid portion of F_j, the feed flow rate of component m, and the total vapor flow rate of the feed, respectively. When F_j is in saturated vapor state, then l_{m,F_j} corresponds to the hypothetical liquid composition that is in thermodynamic equilibrium with the vapor feed.

When two infinite column sections are connected by a sidedraw stream W_j ($j=1,\ldots,N_{\mathrm{W}}$), we denote the section above W_j as $\mathrm{TOP}_{\mathrm{W}j}$ and the one below as $\mathrm{BOT}_{\mathrm{W}j}$. Since $d_i^{\mathrm{TOP}_{\mathrm{W}j}}\leq d_i^{\mathrm{BOT}_{\mathrm{W}j}}$ for every component $i\in\mathcal{C}$, we can show that $p^{\mathrm{TOP}_{\mathrm{W}j}}\geq p^{\mathrm{BOT}_{\mathrm{W}j}}$. Similarly, we define an index set $\mathcal{I}_{\mathrm{W}_j}$ as:

$$\mathcal{I}_{\mathrm{W}_j}=\{i\in\mathcal{C}|\lambda_i^{\mathrm{BOT}_{\mathrm{W}j}}>\lambda_p^{\mathrm{BOT}_{\mathrm{W}j}},\ \lambda_{i-1}^{\mathrm{TOP}_{\mathrm{W}j}}<\lambda_p^{\mathrm{TOP}_{\mathrm{W}j}}\}=\{p^{\mathrm{BOT}_{\mathrm{W}j}}+1,\ldots,p^{\mathrm{TOP}_{\mathrm{W}j}}\}. \tag{6}$$

The feasibility of the target separation in sections $\mathrm{TOP}_{\mathrm{W}j}$ and $\mathrm{BOT}_{\mathrm{W}j}$ requires the following γ root constraint to be satisfied for every $i\in\mathcal{I}_{\mathrm{W}_j}$:

$$\gamma_{i-1}^{\mathrm{TOP}_{\mathrm{W}j}}\leq\rho_{i-1,\mathrm{W}_j}\leq\gamma_i^{\mathrm{BOT}_{\mathrm{W}j}} \qquad \forall i\in\mathcal{I}_{\mathrm{W}_j};\ j=1,\ldots,N_{\mathrm{W}}, \tag{7}$$

where $\{\rho_{i-1,\mathrm{W}_j}\}_{i\in\mathcal{I}_{\mathrm{W}_j}}$ are a subset of solutions of the following equation that is analogous to Equations (5):

$$\sum_{m=1}^{c}\frac{\alpha_m l_{m,\mathrm{W}_j}}{\alpha_m-\rho_{i,\mathrm{W}_j}}=0, \qquad \text{or} \qquad \sum_{m=1}^{c}\frac{\alpha_m f_{m,\mathrm{W}_j}}{\alpha_m-\rho_{i,\mathrm{W}_j}}=V_{\mathrm{W}_j} \qquad i=1,\ldots,c-1;\ j=1,\ldots,N_{\mathrm{W}}, \tag{8}$$

where $\rho_{i,\mathrm{W}_j}\in(\alpha_i,\alpha_{i+1})$. Here, $l_{m,\mathrm{W}_j}\leq 0$, $f_{m,\mathrm{W}_j}\leq 0$, and $V_{\mathrm{W}_j}\leq 0$ correspond to the flow rate of component m in the liquid portion of the sidedraw stream, the sidedraw flow rate of component m, and the total vapor flow rate of the sidedraw, respectively. When W_j is in saturated vapor state, then l_{m,W_j} corresponds to the hypothetical liquid composition that is in thermodynamic equilibrium with the vapor sidedraw.

A unique feature about a sidedraw stream is that the sidedraw's liquid composition (or the hypothetical liquid composition for a vapor-only sidedraw) must belong to the liquid composition profile, whereas a feed's liquid composition (or the hypothetical liquid composition for a vapor-only feed) may or may not belong to the liquid composition profile. Therefore, an additional set of constraints are needed to ensure this for sidedraws. While Equation (7) already takes this aspect into account when $\mathcal{I}_{\mathrm{W}_j}$ is nonempty, we still need to account for a rather common edge case (e.g., Example 2 in Section 5) where $p^{\mathrm{TOP}_{\mathrm{W}j}}=p^{\mathrm{BOT}_{\mathrm{W}j}}$ (note that $p^{\mathrm{TOP}_{\mathrm{W}j}}$ can never be less than $p^{\mathrm{BOT}_{\mathrm{W}j}}$ due to the nature of sidedraw). Let p^{W_j} denote the common pinch index $p^{\mathrm{TOP}_{\mathrm{W}j}}=p^{\mathrm{BOT}_{\mathrm{W}j}}$. The condition that sidedraw composition must belong to the composition profile yields to the following constraint:

$$\begin{aligned}\gamma_i^{\mathrm{TOP}_{\mathrm{W}j}},\gamma_i^{\mathrm{BOT}_{\mathrm{W}j}}&\geq\rho_{i-1,\mathrm{W}_j} \qquad \forall i=p^{\mathrm{W}_j},\ldots,c;\\ \gamma_i^{\mathrm{TOP}_{\mathrm{W}j}},\gamma_i^{\mathrm{BOT}_{\mathrm{W}j}}&\leq\rho_{i,\mathrm{W}_j} \qquad \forall i=1,\ldots,p^{\mathrm{W}_j}-1;\end{aligned} \qquad \forall j=1,\ldots,N_{\mathrm{W}}. \tag{9}$$

3 Formulation of the Minimum Reflux Calculation Algorithm

Now that we have reviewed the key results of our shortcut model, we will derive the formulation to calculate the minimum reflux ratio of a general MFMP column algorithmically. Recall that for a c-component system, the domain of $\gamma_i^{\mathrm{SEC}_k}$ roots to Equation (1) can be split into $c+1$ distinct intervals: $(0, \alpha_1)$, (α_1, α_2), $\ldots$, (α_{c-1}, α_c), and $(\alpha_c, \alpha_c + \delta)$ where δ is a sufficiently large positive number. Based on Equation (2), among these $c+1$ intervals, each of the following $c-1$ intervals must contain at least one root: (α_1, α_2), $\ldots$, (α_{c-1}, α_c). The remaining root, which is the pinch root $\gamma_p^{\mathrm{SEC}_k}$, may lie in one of the $c+1$ intervals depending on whether and where the sign change in $d_i^{\mathrm{SEC}_k}$ occurs (see discussion above).

To model this, for each column section k, we define a set of binary variables $\{\mu_i^{\mathrm{SEC}_k} \in \{0,1\}\}_{i=1}^{c+1}$, where $\mu_i^{\mathrm{SEC}_k} = 1$ when the pinch root $\gamma_p^{\mathrm{SEC}_k} \in (\alpha_{i-1}, \alpha_i)$, and is 0 otherwise. Here, we define $\alpha_0 \coloneqq 0$ and $\alpha_{c+1} \coloneqq \alpha_c + \delta$. This way, the pinch root must satisfy the following constraints:

$$\begin{aligned} &\sum_{i=1}^{c+1} \alpha_{i-1} \mu_i^{\mathrm{SEC}_k} \le \gamma_p^{\mathrm{SEC}_k} \le \sum_{i=1}^{c+1} \alpha_i \mu_i^{\mathrm{SEC}_k} \\ &\sum_{i=1}^{c+1} \mu_i^{\mathrm{SEC}_k} = 1 \end{aligned} \qquad \forall k = 1, \ldots, N_{\mathrm{SEC}}. \tag{10}$$

Next, the nature of feed and sidedraw streams leads to the following sets of constraints for all adjacent column section pairs:

$$\begin{aligned} &\text{Feed stream } \mathrm{F}_j : p^{\mathrm{TOP}_{\mathrm{F}j}} \le p^{\mathrm{BOT}_{\mathrm{F}j}} \Rightarrow \sum_{i=1}^{c+1} i\mu_{i,\mathrm{BOT}_{\mathrm{F}j}} \ge \sum_{i=1}^{c+1} i\mu_{i,\mathrm{TOP}_{\mathrm{F}j}} \quad \forall j = 1, \ldots, N_{\mathrm{F}}; \\ &\text{Sidedraw stream } \mathrm{W}_j : p^{\mathrm{TOP}_{\mathrm{W}j}} \ge p^{\mathrm{BOT}_{\mathrm{W}j}} \Rightarrow \sum_{i=1}^{c+1} i\mu_{i,\mathrm{BOT}_{\mathrm{W}j}} \le \sum_{i=1}^{c+1} i\mu_{i,\mathrm{TOP}_{\mathrm{W}j}} \quad \forall j = 1, \ldots, N_{\mathrm{W}}. \end{aligned} \tag{11}$$

To represent the index sets $\mathcal{I}_{\mathrm{F}}$ and $\mathcal{I}_{\mathrm{W}}$ defined in Equations (3) and (6) in a way that can be implemented algorithmically, we define a new set of binary variables $\{K_i^{\mathrm{SEC}_k} \in \{0,1\}\}_{i=1}^{c+1}$ for column section k where:

$$K_i^{\mathrm{SEC}_k} = \sum_{m=1}^{i} \mu_m^{\mathrm{SEC}_k} \qquad \forall i = 1, \ldots, c+1;\ \forall k = 1, \ldots, N_{\mathrm{SEC}}. \tag{12}$$

Clearly, $K_i^{\mathrm{SEC}_k} = 0$ if and only if $\mu_1^{\mathrm{SEC}_k}, \ldots, \mu_i^{\mathrm{SEC}_k}$ are all equal to 0. And $K_i^{\mathrm{SEC}_k}$ changes from 0 to 1 at index i where $\mu_i^{\mathrm{SEC}_k} = 1$ (i.e., $\gamma_p^{\mathrm{SEC}_k} \in (\alpha_{i-1}, \alpha_i)$) and then stays at 1 for indices greater than i. Now, let us consider two column sections separated by feed stream F_j. For section $\mathrm{TOP}_{\mathrm{F}j}$, the index set $\{i \in \mathcal{C} | \gamma_i^{\mathrm{TOP}_{\mathrm{F}j}} > \gamma_p^{\mathrm{TOP}_{\mathrm{F}j}}\}$ is equivalent to $\{i \in \mathcal{C} | K_{i-1}^{\mathrm{TOP}_{\mathrm{F}j}} = 1\}$. Similarly, for section $\mathrm{BOT}_{\mathrm{F}}j$, the index set $\{i \in \mathcal{C} | \gamma_{i-1}^{\mathrm{BOT}_{\mathrm{F}j}} < \gamma_p^{\mathrm{BOT}_{\mathrm{F}j}}\}$ is the same as $\{i \in \mathcal{C} | K_{i-1}^{\mathrm{BOT}_{\mathrm{F}j}} = 0\}$. Therefore, we can redefine $\mathcal{I}_{\mathrm{F}_j}$ as:

$$\mathcal{I}_{\mathrm{F}_j} = \{i \in \mathcal{C} | K_{i-1}^{\mathrm{TOP}_{\mathrm{F}j}} - K_{i-1}^{\mathrm{BOT}_{\mathrm{F}j}} = 1\} \qquad \forall j = 1, \ldots, N_{\mathrm{F}}. \tag{13}$$

In the example shown in Figure 1, where the root profile corresponds to the column section below a feed stream F_j, $K_1^{\mathrm{BOT}_{\mathrm{F}j}} = K_2^{\mathrm{BOT}_{\mathrm{F}j}} = K_3^{\mathrm{BOT}_{\mathrm{F}j}} = 0$, and $K_4^{\mathrm{BOT}_{\mathrm{F}j}} = K_5^{\mathrm{BOT}_{\mathrm{F}j}} = K_6^{\mathrm{BOT}_{\mathrm{F}j}} = 1$. In terms of the column section above F_j, where $d_1^{\mathrm{TOP}_{\mathrm{F}j}} < 0$ and $d_2^{\mathrm{TOP}_{\mathrm{F}j}}, \ldots, d_5^{\mathrm{TOP}_{\mathrm{F}j}} > 0$, we have $K_1^{\mathrm{TOP}_{\mathrm{F}j}} = 0$, whereas $K_2^{\mathrm{TOP}_{\mathrm{F}j}}$ through $K_6^{\mathrm{TOP}_{\mathrm{F}j}}$ are all equal to 1. Thus, it follows from Equation (13) that $\mathcal{I}_{\mathrm{F}_j} = \{3, 4\}$, which is consistent with what we obtain using Equation (3).

Likewise, the we can redefine $\mathcal{I}_{\mathrm{W}_j}$ as:

$$\mathcal{I}_{\mathrm{W}_j} = \{i \in \mathcal{C} | K_{i-1}^{\mathrm{BOT}_{\mathrm{W}j}} - K_{i-1}^{\mathrm{TOP}_{\mathrm{W}j}} = 1\} \qquad \forall j = 1, \ldots, N_{\mathrm{W}}. \tag{14}$$

This way, we can rewrite Equations (4) and (7) indicating the feasibility of separation in a MFMP column as:

$$\begin{aligned}
&(K_{i-1}^{\mathrm{TOP}_{\mathrm{F}j}} - K_{i-1}^{\mathrm{BOT}_{\mathrm{F}j}})(\gamma_i^{\mathrm{TOP}_{\mathrm{F}j}} - \rho_{i-1,\mathrm{F}_j}) \geq 0 \qquad \forall j = 1, \ldots, N_{\mathrm{F}} \\
&(K_{i-1}^{\mathrm{TOP}_{\mathrm{F}j}} - K_{i-1}^{\mathrm{BOT}_{\mathrm{F}j}})(\rho_{i-1,\mathrm{F}_j} - \gamma_{i-1}^{\mathrm{BOT}_{\mathrm{F}j}}) \geq 0 \qquad \forall j = 1, \ldots, N_{\mathrm{F}} \\
&(K_{i-1}^{\mathrm{BOT}_{\mathrm{W}j}} - K_{i-1}^{\mathrm{TOP}_{\mathrm{W}j}})(\gamma_i^{\mathrm{BOT}_{\mathrm{W}j}} - \rho_{i-1,\mathrm{W}_j}) \geq 0 \qquad \forall j = 1, \ldots, N_{\mathrm{W}} \\
&(K_{i-1}^{\mathrm{BOT}_{\mathrm{W}j}} - K_{i-1}^{\mathrm{TOP}_{\mathrm{W}j}})(\rho_{i-1,\mathrm{W}_j} - \gamma_{i-1}^{\mathrm{TOP}_{\mathrm{W}j}}) \geq 0 \qquad \forall j = 1, \ldots, N_{\mathrm{W}}
\end{aligned} \qquad \forall i = 2, \ldots, c. \tag{15}$$

To implement Equation (9) in an algorithmic fashion, for every $i = 1, \ldots, c+1$ and $j = 1, \ldots, N_{\mathrm{W}}$, we define a binary variables $\omega_i^{\mathrm{W}_j} \coloneqq \mu_m^{\mathrm{TOP}_{\mathrm{W}j}} \mu_m^{\mathrm{BOT}_{\mathrm{W}j}}$, which can be linearized using McCormick envelope. Clearly, $\omega_i^{\mathrm{W}_j} = 1$ when and only when $p^{\mathrm{TOP}_{\mathrm{W}j}} = p^{\mathrm{BOT}_{\mathrm{W}j}}$ (i.e., both pinch roots resides in (α_{i-1}, α_i)). Next, for each sidedraw stream j, we define a set of binary variables $\{H_i^{\mathrm{W}_j}\}_{i=1}^{c+1}$ such that:

$$H_i^{\mathrm{W}_j} = \sum_{m=1}^{i} \omega_m^{\mathrm{W}_j}, \text{ where } \omega_m^{\mathrm{W}_j} \begin{cases} \geq 0 \\ \geq \mu_m^{\mathrm{TOP}_{\mathrm{W}j}} + \mu_m^{\mathrm{BOT}_{\mathrm{W}j}} - 1 \\ \leq \mu_m^{\mathrm{TOP}_{\mathrm{W}j}} \\ \leq \mu_m^{\mathrm{BOT}_{\mathrm{W}j}} \end{cases} \qquad \forall j = 1, \ldots, N_{\mathrm{W}}. \tag{16}$$

Therefore, Equation (9) can be rewritten as:

$$\begin{aligned}
H_i^{\mathrm{W}_j}(\gamma_i^{\mathrm{TOP}_{\mathrm{W}j}} - \rho_{i-1,\mathrm{W}_j}) \geq 0 \qquad &\forall i = 2, \ldots, c; \\
H_i^{\mathrm{W}_j}(\gamma_i^{\mathrm{BOT}_{\mathrm{W}j}} - \rho_{i-1,\mathrm{W}_j}) \geq 0 \qquad &\forall i = 2, \ldots, c; \\
(1 - H_i^{\mathrm{W}_j})(\gamma_i^{\mathrm{TOP}_{\mathrm{W}j}} - \rho_{i,\mathrm{W}_j}) \leq 0 \qquad &\forall i = 1, \ldots, c; \\
(1 - H_i^{\mathrm{W}_j})(\gamma_i^{\mathrm{BOT}_{\mathrm{W}j}} - \rho_{i,\mathrm{W}_j}) \leq 0 \qquad &\forall i = 1, \ldots, c;
\end{aligned} \qquad \forall j = 1, \ldots, N_{\mathrm{W}}. \tag{17}$$

4 Implementation of Minimum Reflux Calculation Algorithm

When implementing the algorithm developed in Section 3, there are two approaches to consider. The first approach is to implement Equations (10), (11), (12), (15), and (17) in an optimization framework as constraints, along with the mathematical formulations of the shortcut model developed in our earlier work[21]. The resulting formulation is a mixed-integer nonlinear program

(MINLP), which can be solved to global optimality using global solvers such as BARON[24]. We use this approach when purity or recovery in product streams are only specified for the light and heavy key components. In this case, the MINLP will determine the optimal distribution of other components in the product streams such that the reflux ratio or reboiler vapor duty requirement is minimized. To illustrate how this approach works, in Section 5.3, we present this formulation for an quaternary separation example in a two-feed, one-sidedraw column.

For many practical applications, the product distributions of the MFMP column have already been fully specified. In this case, the search for minimum reflux ratio of the MFMP column becomes a fully algorithmic procedure that does not require solving an optimization problem. This is because the net material upward flows $\{d_i^{\mathrm{SEC}_k}\}_{i=1}^{c}$ can be readily obtained from mass balances, making the determination of pinch root $\gamma_p^{\mathrm{SEC}_k}$ (and thus the pinch index p^{SEC_k}) completely deterministic following Equation (2) for every column section $k = 1, \ldots, N_{\mathrm{SEC}}$. This means that the index sets $\mathcal{I}_{\mathrm{F}_j}$ and $\mathcal{I}_{\mathrm{W}_j}$ are also fully determined for every feed and sidedraw stream. Therefore, we can run a simple algorithmic procedure presented in Algorithm 1 to identify the true minimum reboiler vapor duty requirement or minimum reflux ratio. Specifically, as discussed in detail in our previous work[21], at minimum reflux condition, one of the feed or sidedraw streams essentially "controls" the separation. Accordingly, the feasibility criteria (Equation (4) or (7)) associated with the controlling feed or sidedraw stream will be satisfied as equalities, whereas the feasibility criteria associated with other streams still need to be satisfied as inequalities. Thus, the idea behind Algorithm 1 is to scrutinize all feed and sidedraw streams, assuming that each of them may be controlling the separation at minimum reflux, and determine whether feasibility criteria are met for all remaining feed and sidedraw streams. Overall, the true reboiler vapor duty (resp. minimum minimum reflux ratio) corresponds to the lowest reboiler vapor duty (resp. lowest reflux ratio) that lead to all feasibility criteria being met.

5 Case Studies

In this section, we examine a few ternary and quanterary separation examples that will illustrate the accuracy and effectiveness of our minimum reflux calculation methods while providing valuable insights of the minimum reflux behavior of a MFMP column for the first time.

5.1 Example 1: Two-Feed Distillation Column

In the first example, we examine a two-feed distillation column shown in Figure 2 separating a ternary mixture of n-hexane (Component 3), n-heptane (Component 2), and n-octane (Component 1). Two-feed columns are common in extractive distillation applications. Furthermore, as recently discovered by Madenoor Ramapriya et al.[25], a large energy saving can potentially be realized when two feed streams are introduced at two different locations of the column compared to pre-mixing them to form a single feed stream.

The relative volatility of each component with respect to octane at atmospheric pressure are estimated from Aspen Plus to be $(\alpha_3, \alpha_2, \alpha_1) = (5.1168, 2.25, 1)$. To establish a common basis for comparison, we ensure constant relative volatility and constant molar overflow assumptions by appropriately modifying the property parameters in Aspen Plus listed under PLXANT and DHVLDP[26]. The IDEAL thermodynamic package is used. This column produces a distillate product with a total flow rate of 52.476 mol/s containing 95 mol% of hexane, 5 mol% of heptane,

input : $\mathcal{C}$, N_{F}, N_{W}, N_{SEC}, $\{f_{i,\mathrm{F}_j}\}_{j=1}^{N_{\mathrm{F}}}$, $\{l_{i,\mathrm{F}_j}\}_{j=1}^{N_{\mathrm{F}}}$, $\{f_{i,\mathrm{W}_j}\}_{j=1}^{N_{\mathrm{W}}}$, $\{l_{i,\mathrm{W}_j}\}_{j=1}^{N_{\mathrm{W}}}$, $d_i^{\mathrm{SEC}_1}$ for every component $i \in \mathcal{C}$

output: minimum reboiler vapor duty $V_{\mathrm{reb,min}}$

initialize: An empty list $\{V_{\mathrm{reb}}\}$ storing candidate minimum reboiler vapor duty values

begin

Calculate $\{d_i^{\mathrm{SEC}_k}\}_{i\in\mathcal{C};\, k=2,\ldots,N_{\mathrm{SEC}}}$ from inter-column section material balances (Equation (29) of Jiang et al.[21]);

From Equation (2), determine all pinch indices and the index sets $\{\mathcal{I}_{\mathrm{F}_j}\}_{j=1}^{N_{\mathrm{F}}}$ and $\{\mathcal{I}_{\mathrm{W}_j}\}_{j=1}^{N_{\mathrm{W}}}$ based on Equations (3) and (6);

Solve Equations (5) and (8) to obtain $\{\rho_{i,\mathrm{F}_j}\}_{i\in\mathcal{C}\setminus\{C\};\, j=1,\ldots,N_{\mathrm{F}}}$ and $\{\rho_{i,\mathrm{W}_j}\}_{i\in\mathcal{C}\setminus\{C\};\, j=1,\ldots,N_{\mathrm{W}}}$, respectively;

for $j \leftarrow 1$ **to** N_{W} **do**

  if $\mathcal{I}_{\mathrm{W}_j} = \emptyset$ **then** Let $p^{\mathrm{W}_j} \leftarrow p^{\mathrm{TOP}_{\mathrm{W}j}}$ and add $V_{\mathrm{reb},\mathrm{W}_j} = \texttt{sidedrawFeasible}(j, p^{\mathrm{W}_j})$ into the list $\{V_{\mathrm{reb}}\}$ **else** Continue;

  for $i \in \mathcal{I}_{\mathrm{W}_j}$ **do**

    Substitute $\gamma_{i-1}^{\mathrm{TOP}_{\mathrm{W}j}} \leftarrow \rho_{i-1,\mathrm{W}_j}$ into Equation (1) to obtain $V^{\mathrm{TOP}_{\mathrm{W}j}}$;

    Add $V_{\mathrm{reb},\mathrm{W}_j} = \texttt{getVreb}(\mathrm{TOP}_{\mathrm{W}j}, V^{\mathrm{TOP}_{\mathrm{W}j}})$ into the list $\{V_{\mathrm{reb}}\}$;

  end

end

for $j \leftarrow 1$ **to** N_{F} **do**

  if $\mathcal{I}_{\mathrm{F}_j} = \emptyset$ **then** Skip and go to the next j **else** Continue;

  for $i \in \mathcal{I}_{\mathrm{F}_j}$ **do**

    Substitute $\gamma_i^{\mathrm{TOP}_{\mathrm{F}j}} \leftarrow \rho_{i-1,\mathrm{F}_j}$ into Equation (1) to obtain $V^{\mathrm{TOP}_{\mathrm{F}j}}$;

    Add $V_{\mathrm{reb},\mathrm{F}_j} = \texttt{getVreb}(\mathrm{TOP}_{\mathrm{F}j}, V^{\mathrm{TOP}_{\mathrm{F}j}})$ into the list $\{V_{\mathrm{reb}}\}$;

  end

end

$V_{\mathrm{reb,min}} = \min\{V_{\mathrm{reb}}\}$

end

Algorithm 1: `Vrebmin`: Algorithm for determining the minimum reboiler vapor duty requirement of a MFMP column knowing the flow rates and compositions of feed and product streams.

input : column section s and its section vapor flow V^{SEC_s}
output: candidate reboiler vapor duty value

begin
  for $k \leftarrow s-1$ **to** 1 **do**
    Calculate V^{SEC_k} from $V^{\mathrm{SEC}_{k+1}}$ via vapor balances;
    Determine $\{\gamma_r^{\mathrm{SEC}_k}\}_{r\in\mathcal{C}}$ from Equation (1) using V^{SEC_k};
    if the feasibility criteria (Equations (4), (7), (9)) associated with SEC_k are satisfied **then** Continue **else return** `null`;
  end
  for $k \leftarrow s+1$ **to** N_{SEC} **do**
    Calculate V^{SEC_k} from $V^{\mathrm{SEC}_{k-1}}$ via vapor balances;
    Determine $\{\gamma_r^{\mathrm{SEC}_k}\}_{r\in\mathcal{C}}$ from Equation (1) using V^{SEC_k};
    if the feasibility criteria (Equations (4), (7), (9)) associated with SEC_k are satisfied **then** Continue **else return** `null`;
  end
  return $V^{\mathrm{SEC}_{N_{\mathrm{SEC}}}}$.
end

Algorithm 2: `getVreb`: Algorithm for checking feasibility of separation and returning the candidate reboiler vapor duty value.

input : sidedraw stream index j, pinch index p^{W_j}
output: candidate reboiler vapor duty value
initialize: An empty list $\{V_{\mathrm{reb,W}_j}\}$ storing candidate minimum reboiler vapor duty values

begin
  for $m \leftarrow 1$ **to** c **do**
    if $m \leq p^{\mathrm{W}_j} - 1$ **then**
      Substitute $\gamma_m^{\mathrm{TOP_{W}}_j} \leftarrow \rho_{m,\mathrm{W}_j}$ into Equation (1) to obtain $V^{\mathrm{TOP_{W}}_j}$; Add $V_{\mathrm{reb},m} = \texttt{getVreb}(\mathrm{TOP_{W}}_j, V^{\mathrm{TOP_{W}}_j})$ into the list $\{V_{\mathrm{reb,W}_j}\}$;
    else if $m \geq p^{\mathrm{W}_j}$ **then**
      Substitute $\gamma_m^{\mathrm{TOP_{W}}_j} \leftarrow \rho_{m-1,\mathrm{W}_j}$ into Equation (1) to obtain $V^{\mathrm{TOP_{W}}_j}$; Add $V_{\mathrm{reb},m} = \texttt{getVreb}(\mathrm{TOP_{W}}_j, V^{\mathrm{TOP_{W}}_j})$ into the list $\{V_{\mathrm{reb,W}_j}\}$;
  end
  return $V^{\mathrm{SEC}_{N_{\mathrm{SEC}}}} \leftarrow \min\{V_{\mathrm{reb,W}_j}\}$.
end

Algorithm 3: `sidedrawFeasible`: Algorithm for returning candidate reboiler vapor duty value "controlled" by sidedraws having the same pinch indices for adjacent column sections.

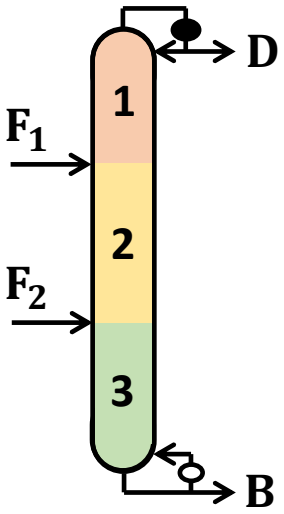

Figure 2: A two-feed column with no sidedraw product stream.

and negligible amount of octane. Thus, bottoms product has a flow rate of 147.524 mol/s containing 0.1 mol% of hexane, 45.671 mol% of heptane, and 54.229 mol% of octane.

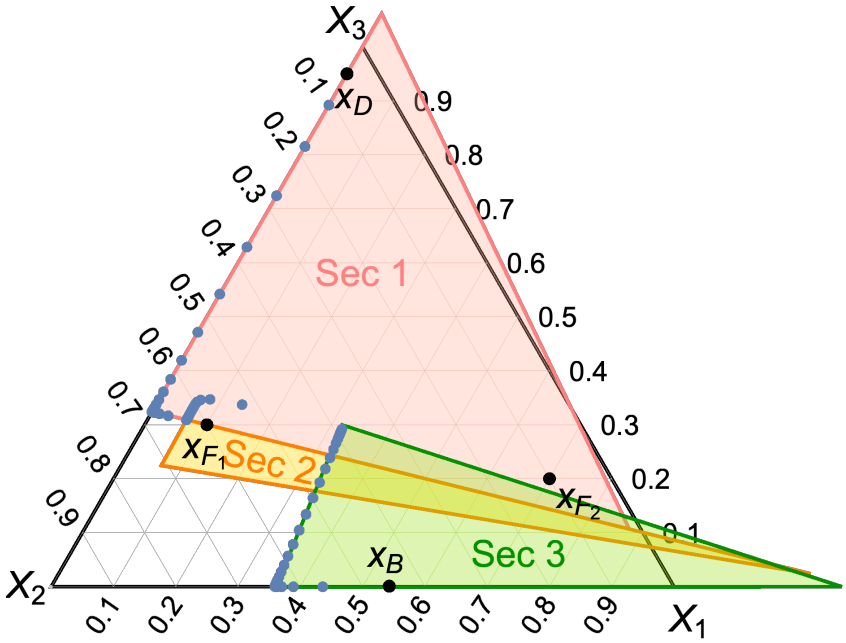

Figure 3: The pinch simplices at the minimum reflux condition obtained using Algorithm 1. Hereafter, X_1, X_2, X_3 represent pure octane, heptane, and hexane, respectively. The blue dots are the actual liquid composition profile of this two-feed column simulated in Aspen Plus as a RadFrac column. By setting up appropriate `Design Specs` in Aspen Plus to simulate the MFMP containing 150 equilibrium stages, we obtain a minimum reflux ratio of $R_{\min} = 2.145$ from Aspen Plus.

We consider two scenarios in Example 1. In the first scenario, the upper feed F_1 in the MFMP column is a saturated liquid stream containing 30 mol/s of hexane, 60 mol/s of heptane, and 10 mol/s of octane. The lower feed F_2 is also a saturated liquid stream but with 20 mol/s of hexane,

10 mol/s of heptane, and 70 mol/s of octane. Clearly, F_2 is less volatile (i.e., "heavier") than F_1 and thus has a higher temperature. Since the feed and product specifications are given, one can directly apply Algorithm 1 to obtain that the minimum reflux ratio $R_{\min} = 2.162$ and the minimum reboiler vapor duty is $V_{\text{reb,min}} = 165.95$ mol/s. The minimum reflux condition occurs when the upper feed F_1 "controls" the separation, where Equation (4) associated with F_1 becomes the binding constraint. To better illustrate this, we construct the pinch simplicies following our previous work[21] for this ternary system at minimum reflux. Following the visualization of Figure 3, the pinch simplices associated with column sections 1 and 2 share a common boundary, where F_1 stream composition $\mathbf{x}_{F_1}$ also lies. This means $z_3^{\text{TOP}_{F1}}(\mathbf{x}_{F_1}) = z_2^{\text{BOT}_{F1}}(\mathbf{x}_{F_1}) = 0$, which implies $\gamma_3^{\text{TOP}_{F1}} = \gamma_2^{\text{BOT}_{F1}} = \rho_{2,F_2}$ (see our previous work[21] for detailed explanation). If the reflux ratio is further reduced, it can be shown that $z_3^{\text{TOP}_{F1}}(\mathbf{x}_{F_1}) < 0$, and $z_2^{\text{BOT}_{F1}}(\mathbf{x}_{F_1}) < 0$, thus violating the feasibility criteria. Geometrically speaking, this implies that the two pinch simplicies will no longer intersect. Therefore, $R_{\min} = 2.162$ is indeed the minimum reflux ratio.

We validate the minimum reflux ratio obtained from our shortcut method using rigorous Aspen Plus simulation. Each column section contains 50 equilibrium stages, much larger than what are needed for this paraffin separation task. This is to ensure that the true minimum reflux condition is achieved. It turns out that the minimum reflux ratio obtained from our shortcut method is less than 1% different compared to true minimum reflux ratio ($R_{\min} = 2.145$) obtained from rigorous Aspen Plus simulation. Also, the liquid composition profile inside the MFMP column at minimum reflux, as shown in Figure 4, exactly follows the behavior of liquid composition trajectory bundle of a pinch simplex. For more details, readers are encouraged to review Sections 3.4 and 4.2 of Jiang et al.[21]. Specifically, since the distillate product is free of octane, the liquid composition profile $\mathbf{x}_n$ (where stage number n is numbered from top to bottom) starting from the distillate product must lie on the hyperplane $z_1^{\text{SEC}_1}(\mathbf{x}) = 0$ until it reaches a (saddle) pinch, which corresponds to a vertex of the pinch simplex and lies somewhere within section 1. Below this pinch, the liquid composition profile continues along the hyperplane $z_3^{\text{SEC}_1}(\mathbf{x}) = 0$ until it reaches the lower end of section 1, which is connected to the top of column section 2. It turns out this is where the pinch zone lies in section 2. Since that the pinch is an unstable node when moving downward along the column, the liquid composition profile moves away from the pinch until it reaches the lower end of section 2. Again, the the pinch zone of section 3 is located at the top of the section, from which the composition profile follows its trajectory inside the pinch simplex and heads toward the stable node until it reaches the bottoms product composition. It is worth noting that, while the hexane composition is small in the bottoms product (0.1 mol%), it is not negligible. Thus, although the liquid composition profile inside section 3 may appear to be approaching to the saddle point pinch, it never actually reaches the saddle pinch, which is clear from Figure 4.

Next, using this example, we would like to examine the prevailing modeling heuristics that (1) a MFMP column can be decomposed into a series of simple columns with exactly one feed and two products, and (2) the actual minimum reflux ratio of the original MFMP column is simply the largest minimum reflux ratio value determined for all decomposed simple columns (which can be determined from the classic Underwood method[27;28]). According to column decomposition, the two-feed column of Figure 2 is modeled as two simple columns, with one having F_1 as the feed stream and consisting of sections 1 and 2, whereas the other with F_2 as the feed stream and consisting of sections 2 and 3. In this case, it turns out that the largest minimum reflux ratio of the two decomposed simple columns is 2.618, which is significantly higher than the true minimum reflux ratio. In other words, the column decomposition approach overestimates the true minimum reflux in this example.

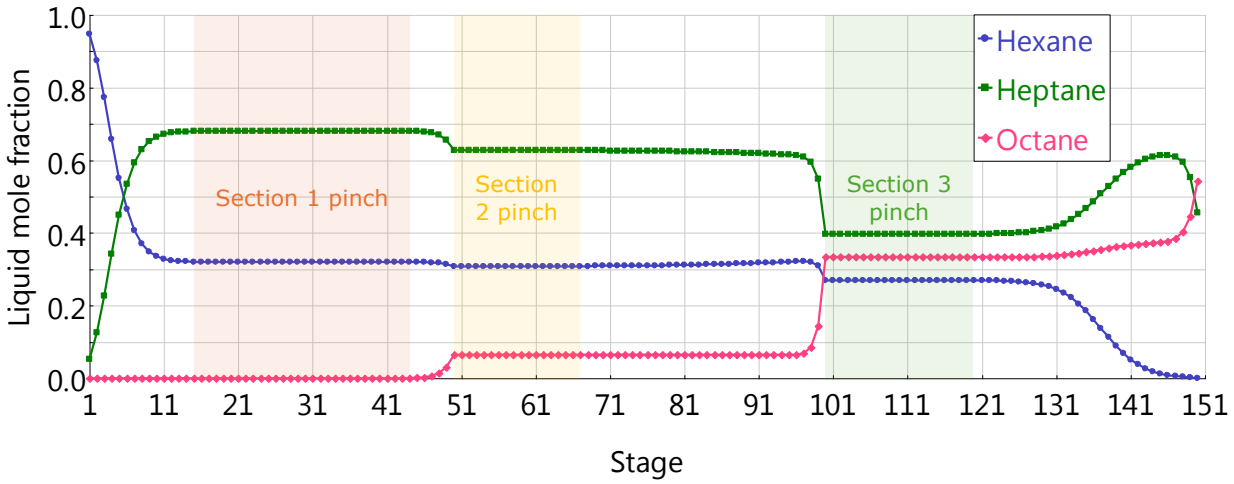

Figure 4: The liquid composition profile retrieved from Aspen Plus at the true minimum reflux ratio of $R_{\min} = 2.145$.

Now, we consider the second scenario where the locations of the two feed streams are switched. In other words, the upper feed F_1 is less volatile than the lower feed F_2. The distillate and bottoms product specifications remain unchanged. Using Algorithm 1, we determine that the minimum reflux ratio of this new arrangement is $R_{\min} = 1.683$. The minimum reflux condition occurs when the lower feed F_2 controls the separation. This can be visualized from the pinch simplex diagram of Figure 5, where sections TOP_{F2} (i.e., section 2) and BOT_{F2} (i.e., section 3) share a common boundary, indicating that $\gamma_3^{\mathrm{TOP}_{F2}} = \gamma_2^{\mathrm{BOT}_{F2}} = \rho_{2,F_2}$.

Rigorous Aspen Plus simulation shows that the true minimum reflux ratio is 1.738. Thus, our shortcut model gives an accurate estimation of the minimum reflux ratio with a 3% relative difference compared to the true minimum reflux ratio. Furthermore, if we adopt the column decomposition method, we would end up with a "minimum reflux ratio" that is as high as 19.714, which is almost 11.3 times as large as the true minimum reflux ratio! Clearly, designing or operating the MFMP column based on incorrect minimum reflux ratio will lead to tremendous capital and operating costs.

By examining the two scenarios, we find that the optimal feed arrangement does not necessarily follow any particular pattern based on its temperature. Intuitively, one might think that, in order to reduce energy consumption (i.e., reflux ratio), feed stream placement should follow the temperature profile. In other words, a high-temperature feed should be placed closer to the bottom of the column than a low-temperature feed. However, it turns out that, despite achieving the same product flow rates and purities, the minimum reflux ratio in the first scenario ($R_{\min} = 2.162$) is much higher than that in the second scenario ($R_{\min} = 1.683$)! While this finding matches with the observation made by Levy and Doherty[29], here we provide a systematic analysis procedure for identifying contradictions of the common belief that a high-temperature feed should be placed below a low-temperature feed. Industrial practitioners should examine carefully the optimal feed arrangement when designing their columns. In this regard, our shortcut model and minimum reflux calculation method allows industrial practitioners to obtain a quick and reliable screening of the optimal feed arrangement.

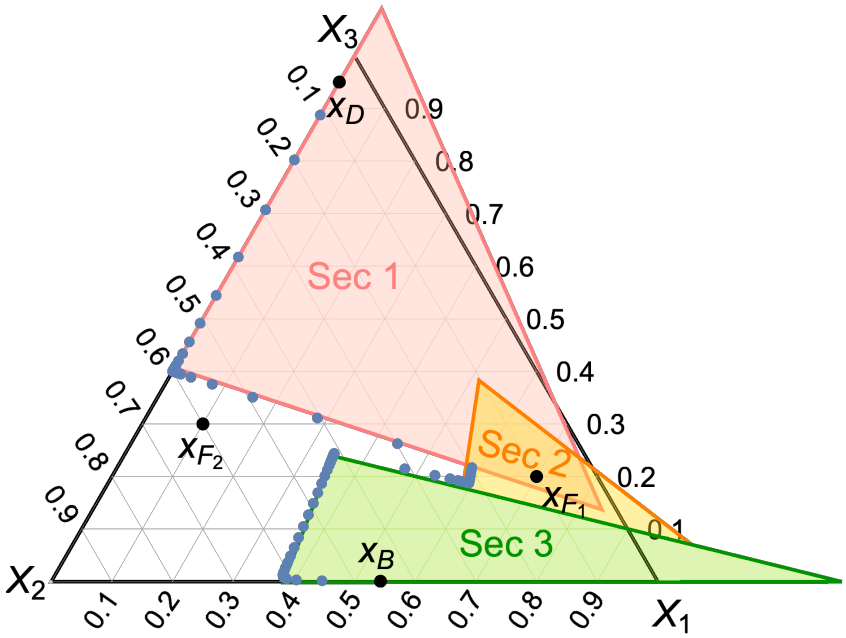

Figure 5: The pinch simplex diagram at calculated minimum reflux ratio of $R_{\min} = 1.683$. The blue dots indicate the liquid composition profile at $R = 1.738$, which is the minimum reflux ratio predicted by rigorous Aspen Plus simulation.

5.2 Example 2: A One-Feed, Two-(Side)Product Column

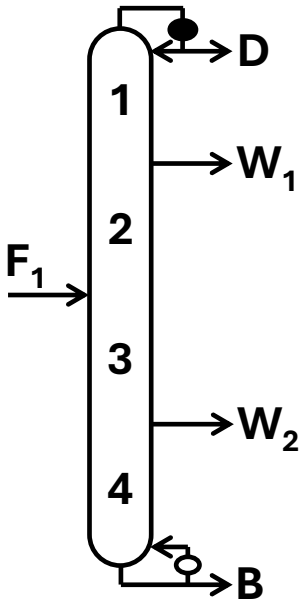

Figure 6: A two-feed column with no sidedraw product stream.

In this example, we study a distillation column separating a ternary mixture of n-hexane, n-heptane, and n-octane with one feed stream and two sidedraw product streams, as shown in Figure 6. When both sidedraw products are withdrawn as saturated liquids, there is a common belief in

the literature (e.g., Sugie and Lu[30], Glinos and Malone[31]) that F_1 will always be "controlling" the separation at minimum reflux. This assumption originates from the observation of the McCabe-Thiele diagram for binary distillation. To verify if this is indeed true for multicomponent distillation, we present this example in which the saturated liquid feed stream F_1 contains 30 mol/s of hexane (Component 3), 40 mol/s of heptane (Component 2), and 30 mol/s of octane (Component 1). The distillate stream contains 24 mol/s of hexane, 6 mol/s of heptane and negligible amount of octane, whereas the bottoms product contains 20 mol/s of octane and no hexane or heptane. The upper sidedraw W_1, which is located above F_1, is a saturated liquid stream with 6 mol/s of hexane and 24 mol/s of heptane. The lower sidedraw W_2 is also a saturated liquid stream with 10 mol/s of heptane and 10 mol/s of octane.

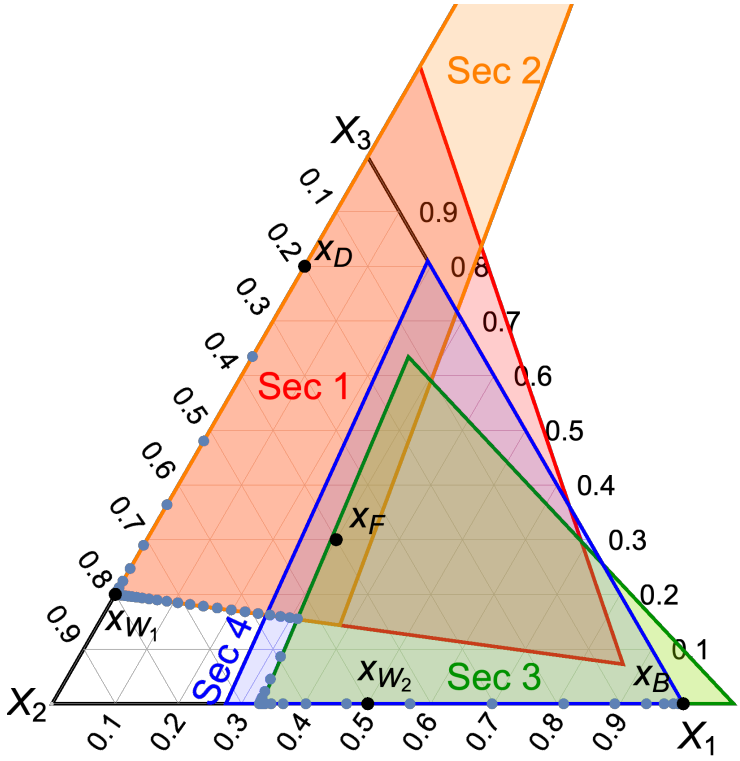

Figure 7: The pinch simplex diagram at the minimum reflux ratio of $R_{\min} = 2.693$, along with the liquid composition profile at the minimum reflux of $R_{\min} = 2.668$ determined by Aspen Plus (see Figure 8 for liquid composition profile).

By applying Algorithm 1, we determine that the minimum reflux ratio is $R_{\min} = 2.693$, which is less than 1% different compared to rigorous Aspen Plus simulation result of 2.668. From the minimum reflux Z-simplex diagram of Figure 7, we can see that it is actually W_1 that controls the separation at minimum reflux. Since $p^{\mathrm{TOP}_{W1}} = p^{\mathrm{BOT}_{W1}} = 2$ (which can be verified from Equation (2) after calculating the net material upward flows for sections 1 and 2), Equation (9) is used to ensures that $\mathbf{x}_{W_1}$ must not be situated outside of the pinch simplices corresponding to sections 1 and 2 as $\mathbf{x}_{W_1}$ must belong to the liquid composition profile. Specifically, at minimum reflux, we have $\gamma_3^{\mathrm{TOP}_{W1}} = \gamma_3^{\mathrm{BOT}_{W1}} = \rho_{2,W_1}$, which is illustrated in Figure 7 where $z_3^{\mathrm{TOP}_{W1}}(\mathbf{x}_{W_1}) = z_3^{\mathrm{BOT}_{W1}}(\mathbf{x}_{W_1}) = 0$. An infinitesimal decrease of reflux ratio will cause facets $z_3^{\mathrm{TOP}_{W1}}(\mathbf{x}) = 0$ and $z_3^{\mathrm{BOT}_{W1}}(\mathbf{x}) = 0$ of pinch simplices to move toward X_3 (pure hexane), hence violating Equation (9).

Assuming that F_1 controls the separation at minimum reflux, then the "minimum reflux ratio"

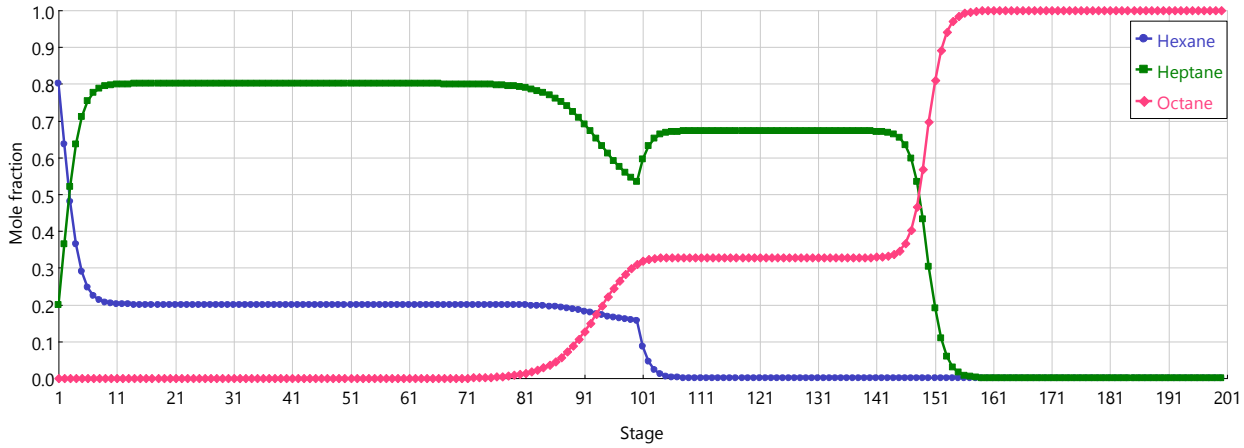

Figure 8: The liquid composition profile retrieved from Aspen Plus at the true minimum reflux ratio $R_{\min} = 2.668$. Each of the four column sections are given 50 equilibrium stages.

calculated under this assumption is 2.533, which turns out to be lower than the true minimum reflux ratio. We have thus provided a counterexample to the common belief that the feed stream always controls the minimum reflux operation when sidedraws are taken as saturated liquid streams. Without incorporating the constraints related to sidedraws (Equations (7), (8), (9), (17)), as what has been done in the literature, one may completely ignore the possibility that a sidedraw could control the separation at minimum reflux and thus will obtain an incorrect minimum reflux ratio value that causes infeasible separation. To the best of our knowledge, this work is the first in deriving these necessary sidedraw-related constraints and incorporating these constraints in a systematic framework to calculate the true minimum reflux ratio. Furthermore, we remark that our proposed minimum reflux calculation method is a generalized framework that is not limited to single-feed columns in saturated liquid sidedraws.

5.3 Example 3: A Two-Feed, One-(Side)Product Column

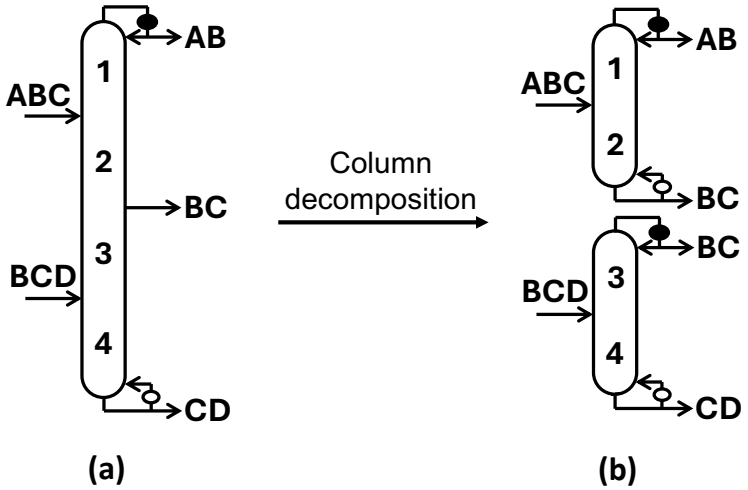

Figure 9: (left) A MFMP column for quaternary separation; (b) the decomposed version of (a).

Now, we study a MFMP column of Figure 9a that separates n-hexane (component A or 4), n-heptane (component B or 3), n-octane (component C or 2), and n-nonane (component D or 1). The relative volatilities with respect to nonane is are $(\alpha_4, \alpha_3, \alpha_2, \alpha_1) = (12.332, 5.361, 2.300, 1)$. Such MFMP columns are very common in multicomponent distillation configurations[4]. In terms of product specifications, the most volatile component A must be completely recovered in the distillate stream, whereas the least volatile component D must be completely recovered in the bottoms product. The distributions of intermediate components B and C in product streams, on the other hand, are flexible. Depending on what the distributions are, the net material upward flow for heptane in column section 2 could be either positive or negative. Similarly, the net material upward flow for octane in column section 3 can be either positive or negative. Therefore, the pinch root in section 2, $\gamma_p^{\mathrm{SEC}_2} = \gamma_3^{\mathrm{SEC}_2}$, lies in the interval $(\alpha_2, \alpha_3) \cup (\alpha_3, \alpha_4)$. Similarly, the pinch root in section 3, $\gamma_p^{\mathrm{SEC}_3} = \gamma_2^{\mathrm{SEC}_3}$, lies in $(\alpha_1, \alpha_2) \cup (\alpha_2, \alpha_3)$. Therefore, we define two binary variables, $\mu_2^{\mathrm{SEC}_2}$ and $\mu_3^{\mathrm{SEC}_2}$, to determine where the pinch root for section 2 lies. We also define two more binary variables, $\mu_1^{\mathrm{SEC}_3}$ and $\mu_2^{\mathrm{SEC}_3}$, for identifying the specific interval where the pinch root for section 3 lies.

Furthermore, since $\gamma_3^{\mathrm{SEC}_2}$ can be in either (α_2, α_3) or (α_3, α_4), and $\gamma_2^{\mathrm{SEC}_3}$ can be in either (α_1, α_2) or (α_2, α_3), singularity issue might arise when implementing Equation (1) in the optimization model when pinch root $\gamma_3^{\mathrm{SEC}_2} = \alpha_3$ and/or when pinch root $\gamma_2^{\mathrm{SEC}_3} = \alpha_2$. To avoid the singularity issue, we reformulate Equation (1) by multiplying both sides of the bound factor (e.g., $(\alpha_3 - \gamma_3^{\mathrm{SEC}_2})$ for V^{SEC_2} expression) followed by performing partial fraction decomposition. For example, the V^{SEC_2} expression can be reformulated as:

$$\begin{aligned} V^{\mathrm{SEC}_2}(\alpha_3 - \gamma_3^{\mathrm{SEC}_2}) &= (\alpha_3 - \gamma_3^{\mathrm{SEC}_2}) \frac{\alpha_2 d_2^{\mathrm{SEC}_2}}{\alpha_2 - \gamma_3^{\mathrm{SEC}_2}} + \alpha_3 d_3^{\mathrm{SEC}_2} \\ &= \alpha_2 d_2^{\mathrm{SEC}_2} + (\alpha_3 - \alpha_2) \frac{\alpha_2 d_2^{\mathrm{SEC}_2}}{\alpha_2 - \gamma_3^{\mathrm{SEC}_2}} + \alpha_3 d_3^{\mathrm{SEC}_2}. \end{aligned}$$

Similarly, we can reformulate the V^{SEC_3} expression using this technique. With this, we can safely bound $\gamma_3^{\mathrm{SEC}_2} \in (\alpha_2, \alpha_4)$ and $\gamma_2^{\mathrm{SEC}_3} \in (\alpha_1, \alpha_3)$ witout concerning about the singularity issue. In Appendix C, we provide all the equations and constraints needed to determine the optimal distribution of intermediate components to minimize the reboiler vapor duty requirement (i.e., V^{SEC_4}) for this MFMP column. The resulting optimization model, which is a mixed-integer nonlinear program (MINLP), can be solved to global optimality quickly using global solvers such as BARON[24]. Specifically, we consider a case where F_1 (ABC) is a saturated vapor stream with 30 mol/s of hexane, 30 mol/s of heptane, and 40 mol/s of octane, whereas F_2 (BCD) is a saturated liquid stream with 40 mol/s of heptane, 30 mol/s of octane, and 30 mol/s of nonane. The sidedraw W_1 (BC) is in saturated liquid state. The lowest possible minimum reboiler vapor duty $V_{\mathrm{reb,min}}$ is determined to be 171.9 mol/s, where its corresponding optimal product distributions summarized in Table 1.

We verify this result by performing exhaustive sensitivity analysis using Aspen Plus. Using rigorous thermodynamic models and tray-by-tray calculations, the lowest reboiler vapor duty requirement that satisfies product requirements is found to be 177.9 mol/s, which is within 5% relative difference compared to the MINLP results. The associated heptane and octane flow rates in product streams also match very well with the results shown in Table 1. This validates the accuracy and computationally efficiency of global optimization framework based on the shortcut model. Moreover, we remark that the global optimization algorithm does more than just finding the minimum energy requirement of a MFMP column and its corresponding product distributions. For example,

Stream	Label	Component flow rate (mol/s)
Distillate	AB	(30, 13.4, 0, 0)
Sidedraw	BC	(0, 56.6, 48.9, 0)
Bottoms	CD	(0, 0, 21.1, 30)

Table 1: Component molar flow rates (arranged as hexane, heptane, octane, and lastly nonane) of all product streams at $V_{\text{reb,min}} = 171.9$ mol/s.

there has been a lingering question among the distillation community of whether all heptane can be recovered from the distillate product in this MFMP column. We can easily answer questions like this by modifying the relevant variable bounds and/or by adding/deactivating related constraints in the MINLP formulation. In this case, when introducing the new constraint $d_3^{\text{SEC}_1} = f_{3,\text{F}_1} + f_{3,\text{F}_2}$, the resulting MINLP problem turns out to be infeasible. Thus, we conclude that it is impossible to recover all the heptane in the distillate product. Rigorous Aspen Plus simulation also confirms that some heptane is always drawn from the sidedraw no matter how much vapor is generated at the reboiler.

Lastly, using this MFMP column as an example, we illustrate why the column decomposition method shown in Figure 9 fails to calculate the true minimum reflux ratio. The feed and product stream specifications in this illustrative case study are listed in Table 2. The minimum reflux ratio calculated using Algorithm 1 is $R_{\min} = 2.002$, which is only 0.1% different from the minimum reflux ratio of 2.000 predicted by Aspen Plus simulation. Furthermore, this is achieved when sidedraw BC controls the minimum reflux condition. Meanwhile, the column decomposition method, which calculates the minimum reflux ratio of two simple columns as shown in Figure 9b using the classic Underwood method, yields a "minimum reflux ratio" of 1.806, which is significantly lower than the true minimum reflux ratio. In fact, as the original MFMP column is decomposed into two simple columns, we lose the possibility that stream BC may control the minimum reflux. Therefore, we must consider the entire MFMP column as a whole to retain all the constraints.

Stream	Component flow rate (mol/s)	Thermal quality
AB	(30, 40, 0, 0)	1
ABC	(30, 30, 40, 0)	0
BC	(0, 30, 40, 0)	1
BCD	(0, 40, 30, 30)	1
CD	(0, 0, 30, 30)	1

Table 2: Component molar flow rates (arranged as hexane, heptane, octane, and lastly nonane) of all streams.

6 Conclusion

In this paper, we introduce the mathematical formulation that incorporates the model developed in the first article of the series[21] to determine the minimum reflux condition of MFMP columns for multicomponent distillation. When the full product specifications are given, an algorithmic procedure is developed to automatically determine the minimum reflux ratio or minimum reboiler

vapor duty requirement. When some of the product specifications are not given to users a priori, an optimization model can be developed as an MINLP to simulatenously identify the minimum reflux ratio and the corresponding optimal product distributions. We present the use of both approaches to analyze the minimum reflux behavior of MFMP columns. In all case studies, our minimum reflux ratio results matches very well with rigorous Aspen Plus simulation results.

In addition to validating the accuracy and usefulness of our proposed algorithmic and optimization frameworks, the second aim of these case studies is to reexamine some of the well-accepted design heuristics and modeling assumptions the distillation community has been relying on regarding how MFMP columns should be designed and operated. It turns out that some of these heuristics and assumptions need to be rewritten. In Example 1, we show a counterexample where placing a colder feed stream above a warmer feed stream, which follows the temperature profile within the column, actually leads to a higher minimum vapor duty requirement than if the feed stream locations are reversed. Thus, we must analyze all possible permutations of relative feed locations to determine the optimal feed stream arrangement. Our shortcut based approach is particularly suitable for analyses like this compared to rigorous process simulations which can be quite time consuming to perform, especially as the number of feed streams and/or sidedraw streams increases.

Another key finding is that decomposing a MFMP column into multiple simple columns and taking the largest individual minimum reflux ratios of each decomposed column using the classic Underwood method is not the correct approach to determine the minimum reflux ratio of the original MFMP column. In fact, such column decomposition approach can lead to minimum reflux ratio values that significantly deviate from the true minimum reflux ratio. On the other hand, our shortcut based approach considers the entire MFMP column as a whole, which is needed for accurately estimating the true minimum reflux ratio.

Finally, when a distillation column has one or more sidedraw streams, one of the sidedraw streams can control the separation at minimum reflux, even when they are all withdrawn as saturated liquid streams. This possibility has often been overlooked by the distillation community in the past due to the lack of fundamental understanding and systematic tools to model how sidedraws affect the minimum reflux operation of a column. The mathematical model and algorithms developed in this series have filled this gap, thus allowing industrial practitioners to conduct rigorous, accurate analysis of columns with sidedraws for the first time. Overall, we believe that these new findings and insights are helpful in synthesizing and operating energy-efficient, cost-competitive, and intensified MFMP columns for multicomponent distillation.

Acknowledgment

The information, data, or work presented herein was funded in part by the Office of Energy Efficiency and Renewable Energy (EERE), U.S. Department of Energy, under Award Number DE-EE0005768.

References

1 Górak A, Olujić Z. Distillation: Fundamentals and Principles. Elsevier Inc. 2014.

2 US DOE Industrial Efficiency & Decarbonization Office. Manufacturing Energy and Carbon Footprints (2018 MECS). 2021.

3 US DOE. Industrial Decarbonization Roadmap. 2022.

4 Shah VH, Agrawal R. A matrix method for multicomponent distillation sequences. AIChE Journal. 2010;56(7):1759–1775.

5 Nallasivam U, Shah VH, Shenvi AA, Tawarmalani M, Agrawal R. Global optimization of multicomponent distillation configurations: 1. Need for a reliable global optimization algorithm. AIChE Journal. 2013;59(3):971–981.

6 Nallasivam U, Shah VH, Shenvi AA, Huff J, Tawarmalani M, Agrawal R. Global optimization of multicomponent distillation configurations: 2. Enumeration based global minimization algorithm. AIChE Journal. 2016;62(6):2071–2086.

7 Jiang Z, Agrawal R. Process intensification in multicomponent distillation: A review of recent advancements. Chemical Engineering Research and Design. 2019;147:122–145.

8 Jiang G Zheyuand Madenoor Ramapriya, Tawarmalani M, Agrawal R. Process intensification in multicomponent distillation. Chemical Engineering Transactions. 2018;69:841–846.

9 Agrawal R, Tumbalam Gooty R. Misconceptions about efficiency and maturity of distillation. AIChE Journal. 2020;66(8):e16294.

10 Agrawal R, Yee TF. Heat Pumps for Thermally Linked Distillation Columns: An Exercise for Argon Production from Air. Industrial & Engineering Chemistry Research. 1994;33(11):2717–2730.

11 Nogaja A, Tawarmalani M, Agrawal R. Distillation Electrification Through Optimal Use of Heat Pumps. In: 34th European Symposium on Computer Aided Process Engineering / 15th International Symposium on Process Systems Engineering, edited by Manenti F, Reklaitis GV, vol. 53 of Computer Aided Chemical Engineering, pp. 1297–1302. Elsevier. 2024;.

12 Wankat PC. Multieffect distillation processes. Industrial & Engineering Chemistry Research. 1993;32(5):894–905.

13 Agrawal R, Herron DM. Intermediate reboiler and condenser arrangement for binary distillation columns. AIChE Journal. 1998;44(6):1316–1324.

14 Agrawal R, Fidkowski ZT, Xu J. Prefractionation to reduce energy consumption in distillation without changing utility temperatures. AIChE Journal. 1996;42(8):2118–2127.

15 Agrawal R, Herron DM. Optimal thermodynamic feed conditions for distillation of ideal binary mixtures. AIChE Journal. 1997;43(11):2984–2996.

16 Jiang Z, Madenoor Ramapriya G, Tawarmalani M, Agrawal R. Minimum energy of multicomponent distillation systems using minimum additional heat and mass integration sections. AIChE Journal. 2018;64(9):3410–3418.

17 Tumbalam Gooty R, Chavez Velasco JA, Agrawal R. Methods to assess numerous distillation schemes for binary mixtures. Chemical Engineering Research and Design. 2021;172:1–20.

18 Chavez Velasco JA, Tawarmalani M, Agrawal R. Systematic Analysis Reveals Thermal Separations Are Not Necessarily Most Energy Intensive. Joule. 2021;5(2):330–343.

19 Gilliland ER. MULTICOMPONENT RECTIFICATION. Industrial & Engineering Chemistry. 1940;32(8):1101–1106.

20 Doherty MF. Conceptual design of distillation systems. McGraw-Hill chemical engineering series. Boston: McGraw-Hill. 2001.

21 Jiang Z, Tawarmalani M, Agrawal R. Minimum reflux calculation for multicomponent distillation in multi-feed, multi-product columns: Mathematical model. AIChE Journal. 2022; 68(12):e17929.

22 Jiang Z, Mathew TJ, Zhang H, Huff J, Nallasivam U, Tawarmalani M, Agrawal R. Global optimization of multicomponent distillation configurations: Global minimization of total cost for multicomponent mixture separations. Computers & Chemical Engineering. 2019;126:249–262.

23 Jiang Z, Chen Z, Huff J, Shenvi AA, Tawarmalani M, Agrawal R. Global minimization of total exergy loss of multicomponent distillation configurations. AIChE Journal. 2019;65(11):e16737.

24 Tawarmalani M, Sahinidis NV. A polyhedral branch-and-cut approach to global optimization. Mathematical Programming. 2005;103:225–249.

25 Madenoor RG, Mohit T, Rakesh A. Modified basic distillation configurations with intermediate sections for energy savings. AIChE Journal. 2014;60(3):1091–1097.

26 Shah VH. Energy savings in distillation via identification of useful configurations. Ph.D. thesis, Purdue University. 2010.

27 Underwood AJV. Fractional Distillation of Multicomponent Mixtures. Industrial & Engineering Chemistry. 1949;41(12):2844–2847.

28 Underwood AJV. Fractional distillation of multicomponent mixtures. Chemical Engineering Progress. 1948;44:603–614.

29 Levy SG, Doherty MF. Design and synthesis of homogeneous azeotropic distillations. 4. Minimum reflux calculations for multiple-feed columns. Industrial & Engineering Chemistry Fundamentals. 1986;25(2):269–279.

30 Sugie H, Lu B. On the determination of minimum reflux ratio for a multicomponent distillation column with any number of side-cut streams. Chemical Engineering Science. 1970;25(12):1837–1846.

31 Glinos KN, Malone MF. Design of sidestream distillation columns. Industrial & Engineering Chemistry Process Design and Development. 1985;24(3):822–828.

Appendix A: Parameters and Variables

c	Total number of components present in the distillation column
α_i	Relative volatility of component i with respect to the heaviest component
$d_i^{\mathrm{SEC}_k}$	Component i's net material upward flow in column section k
V^{SEC_k}	Total vapor flow in column section k
$\gamma_i^{\mathrm{SEC}_k}$	The i^{th} root of Equation (1)
p^{SEC_k}	The pinch index of section k
$\gamma_p^{\mathrm{SEC}_k}$	The pinch root of section k
$\mathbf{x}$	The liquid composition vector
X_i	The composition of pure component i
$\mathbf{x}_{\mathrm{F}}$	Liquid composition (or hypothetical liquid composition) composition of feed stream
$\mathbf{x}_{\mathrm{W}}$	Liquid composition (or hypothetical liquid composition) of sidedraw stream
$\rho_{i,\mathrm{F}}$, $\rho_{i,\mathrm{W}}$	The i^{th} root defined in Equations (5) and (8), respectively
V_{F}, V_{W}	Total vapor flow rate in feed and sidedraw stream, respectively
$f_{i,\mathrm{F}}$, $f_{i,\mathrm{W}}$	Component i's flow rate in feed and sidedraw stream, respectively
N_{F}	Number of feed streams in the column
N_{W}	Number of sidedraw streams in the column
N_{SEC}	Number of column sections in the column, which is equal to $N_{\mathrm{F}} + N_{\mathrm{W}} + 1$
$\mu_i^{\mathrm{SEC}_k}$	Binary variable that equals 1 when $\gamma_p^{\mathrm{SEC}_k} \in (\alpha_{i-1}, \alpha_i)$, and 0 otherwise
$K_i^{\mathrm{SEC}_k}$	Binary variable defined in Equation (12) and used in Equations (15) and (17)
$H_i^{\mathrm{W}_j}$	Binary variable defined in Equation (16) and used in Equation (17)

Appendix B: Sets and Notations

$\mathcal{C}$	$\{1, \cdots, c\}$
$\mathcal{I}_{\mathrm{F}}$	Index set defined in Equation (3) for feasibility criteria associated with feed streams
$\mathcal{I}_{\mathrm{W}}$	Index set defined in Equation (6) for feasibility criteria associated with sidedraws
$\mathrm{TOP}_{\mathrm{F}}$	Column section above a feed stream
$\mathrm{BOT}_{\mathrm{F}}$	Column section below a feed stream
$\mathrm{TOP}_{\mathrm{W}}$	Column section above a sidedraw stream, respectively
$\mathrm{BOT}_{\mathrm{W}}$	Column section below a sidedraw stream, respectively
F, W	Feed and sidedraw stream, respectively

Appendix C: Optimization Model

Here, we provide the complete formulation for identifying the minimum reboiler vapor duty and the corresponding product distributions for the column shown in Figure 2.

Objective function:

$$\text{minimize } V^{\mathrm{SEC}_4}$$

Constraints and bounds:

1. Mass balance equations and feed specifications:

$$f_{i,\mathrm{F}_1} + f_{i,\mathrm{F}_2} = d_i^{\mathrm{SEC}_1} - f_{i,\mathrm{W}_1} - d_i^{\mathrm{SEC}_4} \qquad \forall i = 1,\ldots,4$$
$$d_i^{\mathrm{SEC}_2} = d_i^{\mathrm{SEC}_1} - f_{i,\mathrm{F}_1};\ d_i^{\mathrm{SEC}_3} = d_i^{\mathrm{SEC}_2} - f_{i,\mathrm{W}_1}; d_i^{\mathrm{SEC}_4} = d_i^{\mathrm{SEC}_3} - f_{i,\mathrm{F}_2} \qquad \forall i = 1,\ldots,4$$
$$f_{4,\mathrm{F}_1} = d_4^{\mathrm{SEC}_1} = 30;\ f_{1,\mathrm{F}_2} = -d_1^{\mathrm{SEC}_4} = 30$$
$$f_{3,\mathrm{F}_1} = 30;\ f_{2,\mathrm{F}_1} = 40;\ f_{1,\mathrm{F}_1} = 0;\ f_{4,\mathrm{F}_2} = 0;\ f_{3,\mathrm{F}_2} = 40;\ f_{2,\mathrm{F}_2} = 30;$$
$$f_{i,\mathrm{F}_j} \geq 0 \qquad \forall i = 1,\ldots,4;\ j = 1,2$$
$$d_i^{\mathrm{SEC}_1} \geq 0;\ f_{i,\mathrm{W}_1} \leq 0;\ d_i^{\mathrm{SEC}_4} \leq 0 \qquad \forall i = 1,\ldots,4$$

2. Vapor duty calculation based on Equation (1):

$$V^{\mathrm{SEC}_1} = \sum_{i=1}^{4} \frac{\alpha_i d_i^{\mathrm{SEC}_1}}{\alpha_i - \gamma_4^{\mathrm{SEC}_1}}$$
$$V^{\mathrm{SEC}_1} = \sum_{i=1}^{4} \frac{\alpha_i d_i^{\mathrm{SEC}_1}}{\alpha_i - \gamma_3^{\mathrm{SEC}_1}}$$
$$V^{\mathrm{SEC}_2}(\alpha_3 - \gamma_3^{\mathrm{SEC}_2}) = \alpha_2 d_2^{\mathrm{SEC}_2} + (\alpha_3 - \alpha_2)\frac{\alpha_2 d_2^{\mathrm{SEC}_2}}{\alpha_2 - \gamma_3^{\mathrm{SEC}_2}} + \alpha_3 d_3^{\mathrm{SEC}_2}$$
$$V^{\mathrm{SEC}_2} = \sum_{i=1}^{4} \frac{\alpha_i d_i^{\mathrm{SEC}_2}}{\alpha_i - \gamma_2^{\mathrm{SEC}_2}}$$
$$V^{\mathrm{SEC}_3}(\alpha_2 - \gamma_2^{\mathrm{SEC}_3}) = \alpha_2 d_2^{\mathrm{SEC}_3} - (\alpha_3 - \alpha_2)\frac{\alpha_3 d_3^{\mathrm{SEC}_3}}{\alpha_3 - \gamma_2^{\mathrm{SEC}_3}} + \alpha_3 d_3^{\mathrm{SEC}_3}$$
$$V^{\mathrm{SEC}_3} = \sum_{i=1}^{4} \frac{\alpha_i d_i^{\mathrm{SEC}_3}}{\alpha_i - \gamma_3^{\mathrm{SEC}_3}}$$
$$V^{\mathrm{SEC}_4} = \sum_{i=1}^{4} \frac{\alpha_i d_i^{\mathrm{SEC}_4}}{\alpha_i - \gamma_1^{\mathrm{SEC}_4}}$$
$$V^{\mathrm{SEC}_4} = \sum_{i=1}^{4} \frac{\alpha_i d_i^{\mathrm{SEC}_4}}{\alpha_i - \gamma_2^{\mathrm{SEC}_4}}$$

3. Defining equations for the feed and sidedraw streams:

$$V_{\mathrm{F}_1} = 100 = \sum_{i=1}^{4} \frac{\alpha_i f_{i,\mathrm{F}_1}}{\alpha_i - \rho_{j,\mathrm{F}_1}} \qquad \forall j = 1,\ldots,3$$
$$V_{\mathrm{F}_2} = 0 = \sum_{i=1}^{4} \frac{\alpha_i f_{i,\mathrm{F}_2}}{\alpha_i - \rho_{j,\mathrm{F}_2}} \qquad \forall j = 1,\ldots,3$$
$$V_{\mathrm{W}_1} = 0 = \sum_{i=1}^{4} \frac{\alpha_i f_{i,\mathrm{W}_1}}{\alpha_i - \rho_{j,\mathrm{W}_1}} \qquad \forall j = 1,\ldots,3$$

4. Variable bounds:

$$\gamma_3^{\mathrm{SEC}_1} \in (\alpha_2, \alpha_3);\ \gamma_4^{\mathrm{SEC}_1} \in (\alpha_3, \alpha_4)$$
$$\gamma_2^{\mathrm{SEC}_2} \in (\alpha_2, \alpha_3);\ \gamma_3^{\mathrm{SEC}_2} \in (\alpha_2, \alpha_4)$$
$$\gamma_2^{\mathrm{SEC}_3} \in (\alpha_1, \alpha_3);\ \gamma_3^{\mathrm{SEC}_3} \in (\alpha_2, \alpha_3)$$
$$\gamma_1^{\mathrm{SEC}_4} \in (\alpha_1, \alpha_2);\ \gamma_2^{\mathrm{SEC}_4} \in (\alpha_2, \alpha_3)$$
$$\rho_{i,\mathrm{F}_1},\ \rho_{i,\mathrm{F}_2},\ \rho_{i,\mathrm{W}_1} \in (\alpha_i, \alpha_{i+1}) \qquad \forall i = 1, \ldots, 3$$

5. Defining binary variables μ:

$$\mu_2^{\mathrm{SEC}_2},\ \mu_3^{\mathrm{SEC}_2},\ \mu_1^{\mathrm{SEC}_3},\ \mu_2^{\mathrm{SEC}_3} \in \{0, 1\}$$
$$\mu_2^{\mathrm{SEC}_2} + \mu_3^{\mathrm{SEC}_2} = 1;\ \mu_1^{\mathrm{SEC}_3} + \mu_2^{\mathrm{SEC}_3} = 1$$

6. Feasibility criteria:

$$\alpha_2\mu_2^{\mathrm{SEC}_2} + \alpha_3\mu_3^{\mathrm{SEC}_2} \leq \gamma_3^{\mathrm{SEC}_2} \leq \alpha_3\mu_2^{\mathrm{SEC}_2} + \alpha_4\mu_3^{\mathrm{SEC}_2}$$
$$\alpha_1\mu_1^{\mathrm{SEC}_3} + \alpha_2\mu_2^{\mathrm{SEC}_3} \leq \gamma_2^{\mathrm{SEC}_3} \leq \alpha_2\mu_1^{\mathrm{SEC}_3} + \alpha_3\mu_2^{\mathrm{SEC}_3}$$
$$\gamma_2^{\mathrm{SEC}_1} \geq \gamma_1^{\mathrm{SEC}_2};\ \gamma_3^{\mathrm{SEC}_1} \geq \gamma_2^{\mathrm{SEC}_2};\ (1 - \mu_2^{\mathrm{SEC}_2})(\gamma_4^{\mathrm{SEC}_1} - \gamma_3^{\mathrm{SEC}_2}) \geq 0$$
$$\mu_1^{\mathrm{SEC}_3}(\gamma_2^{\mathrm{SEC}_3} - \gamma_1^{\mathrm{SEC}_2}) \geq 0;\ \gamma_3^{\mathrm{SEC}_3} \geq \gamma_2^{\mathrm{SEC}_2};\ (1 - \mu_2^{\mathrm{SEC}_2})(\gamma_4^{\mathrm{SEC}_3} - \gamma_3^{\mathrm{SEC}_2}) \geq 0$$
$$\mu_1^{\mathrm{SEC}_3}(\gamma_2^{\mathrm{SEC}_3} - \gamma_1^{\mathrm{SEC}_4}) \geq 0;\ \gamma_3^{\mathrm{SEC}_3} \geq \gamma_2^{\mathrm{SEC}_4};\ \gamma_4^{\mathrm{SEC}_3} \geq \gamma_3^{\mathrm{SEC}_4}$$
$$\mu_2^{\mathrm{SEC}_2}(\gamma_3^{\mathrm{SEC}_2} - \theta_{2,\mathrm{W}_1}) \geq 0;\ \gamma_2^{\mathrm{SEC}_2} \leq \theta_{2,\mathrm{W}_1}$$
$$\gamma_3^{\mathrm{SEC}_3} \geq \theta_{2,\mathrm{W}_1};\ (1 - \mu_1^{\mathrm{W}_3})(\gamma_2^{\mathrm{SEC}_3} - \theta_{2,\mathrm{W}_1}) \leq 0$$